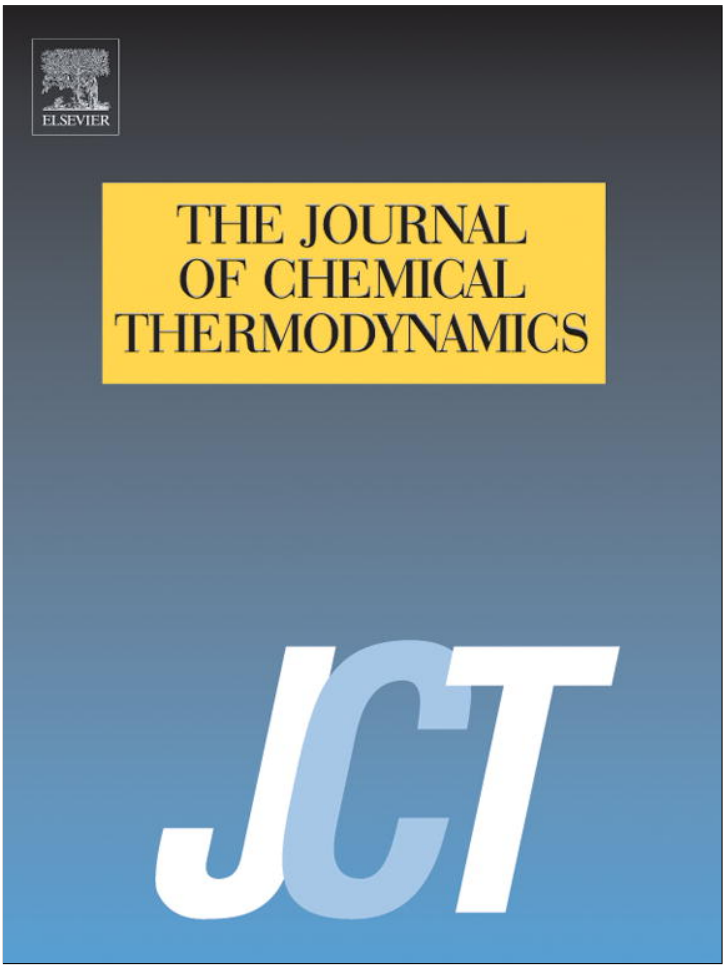

(This is a sample cover image for this issue. The actual cover is not yet available at this time.)

J. Chem. Thermodynamics 60 (2013) 41–45

Contents lists available at SciVerse ScienceDirect

J. Chem. Thermodynamics

journal homepage: www.elsevier.com/locate/jct

The curvature of the liquid–vapor reduced pressure curve and its relation with the critical region

S. Velasco [a,b], M.J. Santos [a], J.A. White [a,b,*], K. Srinivasan [c,d]

[a] Departamento de Física Aplicada, Universidad de Salamanca, 37008 Salamanca, Spain
[b] IUFFyM, Universidad de Salamanca, 37008 Salamanca, Spain
[c] Department of Mechanical Engineering, Indian Institute of Science, Bangalore 560012, India
[d] Department of Mechanical Engineering, University of Melbourne, Vic 3010, Australia

ARTICLE INFO

Article history:
Received 20 November 2012
Received in revised form 14 January 2013
Accepted 18 January 2013
Available online 29 January 2013

Keywords:
Vapor pressure curve
Saturation properties
Critical behavior
Curvature

ABSTRACT

For most fluids, there exist a maximum and a minimum in the curvature of the reduced vapor pressure curve, $p_r = p_r(T_r)$ (with $p_r = p/p_c$ and $T_r = T/T_c$, p_c and T_c being the pressure and temperature at the critical point). By analyzing National Institute of Standards and Technology (NIST) data on the liquid-vapor coexistence curve for 105 fluids, we find that the maximum occurs in the reduced temperature range $0.5 \leqslant T_r \leqslant 0.8$ while the minimum occurs in the reduced temperature range $0.980 \leqslant T_r \leqslant 0.995$. Vapor pressure equations for which d^2p_r/dT_r^2 diverges at the critical point present a minimum in their curvature. Therefore, the point of minimum curvature can be used as a marker for the critical region. By using the well-known Ambrose–Walton (AW) vapor pressure equation we obtain the reduced temperatures of the maximum and minimum curvature in terms of the Pitzer acentric factor. The AW predictions are checked against those obtained from NIST data.

1. Introduction

Some years ago, Srinivasan [1] proposed the study of the curvature (inverse of the radius of curvature) as a way of characterizing the reduced vapor pressure curve. This curvature is defined as

$$k = \frac{\mathrm{d}^2 p_r/\mathrm{d}T_r^2}{\left[1 + (\mathrm{d}p_r/\mathrm{d}T_r)^2\right]^{3/2}}, \tag{1}$$

where $p_r = p/p_c$ is the reduced vapor pressure and $T_r = T/T_c$ the reduced temperature, p_c and T_c being the pressure and temperature at the critical point. The derivatives appearing in equation (1) can be experimentally obtained from the Clapeyron equation

$$\frac{p_c}{T_c}\frac{\mathrm{d}p_r}{\mathrm{d}T_r} = \frac{\mathrm{d}p}{\mathrm{d}T} = \frac{\Delta_v h}{T(v^g - v^l)} \tag{2}$$

and the Yang–Yang equation [2]

$$\frac{p_c}{T_c^2}\frac{\mathrm{d}^2 p_r}{\mathrm{d}T_r^2} = \frac{\mathrm{d}^2 p}{\mathrm{d}T^2} = \frac{c_{v2}^g - c_{v2}^l}{T(v^g - v^l)}, \tag{3}$$

where $\Delta_v h$ is the specific enthalpy of vaporization, v^g and v^l are the vapor (g) and liquid (l) specific volumes at saturation, and c_{v2}^g and c_{v2}^l are the two-phase vapor and liquid specific heat capacities at constant volume. Alternatively, the first and second derivatives of the reduced vapor pressure can be obtained from vapor pressure data either numerically or from a given functional form of the vapor pressure equation.

By analyzing vapor pressure data of 17 fluids consisting of several refrigerants, carbon dioxide, cryogenic liquids and water, Srinivasan [1] observed the existence of a maximum in the curvature (1) for all the considered fluids (except carbon dioxide), in the reduced temperature range $0.6 \leqslant T_r \leqslant 0.7$. Furthemore, Srinivasan [1] also observed the existence of a minimum in the curvature (1) near the critical point for most, but not for all, of the considered fluids. Practical implications of these features for the choice of working fluids in vapor pressure thermometry and in sensor bulbs of the thermostatic expansion valves used in engineering systems were also discussed by Srinivasan in his work [1].

In the present work we extend Srinivasan's study by analyzing the curvature of the vapor pressure curve by using liquid-vapor coexistence data for 105 pure fluids reported by the National Institute of Standards and Technology (NIST) program RefProp. 9.0 [3]. This extension allows us to enlarge the range for the reduced temperature of the maximum curvature reported by Srinivasan and to show that this reduced temperature is well-correlated with the Pitzer acentric factor ω. We also analyze the occurrence of a minimum in the curvature of the reduced vapor pressure curve close to the critical point. Indeed, this minimum occurs in the reduced temperature range $0.980 \leqslant T_r \leqslant 0.995$, but some of the considered

* Corresponding author at: Departamento de Física Aplicada, Universidad de Salamanca, 37008 Salamanca, Spain. Tel.: +34 923294436; fax: +34 923294584.
E-mail address: white@usal.es (J.A. White).

0021-9614/$ - see front matter © 2013 Elsevier Ltd. All rights reserved.
http://dx.doi.org/10.1016/j.jct.2013.01.014

fluids do not present this minimum. However, by analyzing theoretically the curvature (1) near the critical point we conclude that this minimum must exist for any fluid. This implies that this minimum can be observed only when a thermodynamically consistent vapor pressure equation is chosen. We analyze the case of the Ambrose–Walton vapor pressure equation as a paradigmatic equation in the Pitzer corresponding-states scheme.

2. Curvature far the critical point

Far enough the critical point one can assume that $\Delta_v h \approx$ const and $v^l \ll v^g \approx RT/p$. Under these assumptions, by taking as reference the acentric point ($T_r = 0.7$), integration of equation (2) leads to the Clausius–Clapeyron (CC) equation [4]

$$\ln p_r = A(\omega)\left(1 - \frac{1}{T_r}\right), \tag{4}$$

with

$$A(\omega) = \frac{7 \ln 10}{3}(1+\omega), \tag{5}$$

where ω is the so-called Pitzer acentric factor defined by Pitzer *et al.* [5]

$$\omega = -1.0 - \log_{10} p_r \quad \text{at} \quad T_r = 0.7. \tag{6}$$

From equation (4), one obtains

$$\frac{dp_r}{dT_r} = \frac{A(\omega)}{T_r^2} p_r \tag{7}$$

and

$$\frac{d^2 p_r}{dT_r^2} = \left[\frac{A(\omega)}{T_r} - 2\right]\frac{A(\omega)}{T_r^3} p_r, \tag{8}$$

with p_r given by equation (4). Figure 1(a) and (b) show, respectively, the first and second derivatives of the reduced vapor pressure for propane. Symbols correspond to equations (2) and (3) with $\Delta_v h$, v^g, v^l, c_{v2}^g and c_{v2}^l data obtained from RefProp 9.0 [3]. Dashed lines correspond to equations (7) and (8) with $\omega = 0.1521$, the value of the acentric factor for propane [3]. One can see that the CC equations (7) and (8) reproduce fairly well the NIST data far away the critical point.

Substitution of equations (7) and (8) into equation (1) yields

$$k^{CC} = A(\omega) p_r T_r^2 \frac{A(\omega) - 2T_r}{\left[T_r^4 + A(\omega)^2 p_r^2\right]^{3/2}} \tag{9}$$

for the curvature of the CC equation. The curvature for propane in the range $0.3 \leqslant T_r \leqslant 0.95$ using equation (9) with $\omega = 0.1521$ is plotted in figure 2(a) by a dashed line, showing a maximum at $T_{r,\max} = 0.6543$. Figure 2(a) also shows (symbols) the curvature for propane using equations (1)–(3) and $\Delta_v h$, v^g, v^l, c_{v2}^g and c_{v2}^l data obtained from RefProp 9.0, in the reduced temperature range $0.3 \leqslant T_r \leqslant 0.95$. This curvature presents a maximum at $T_{r,\max} = 0.6505$, close to the value obtained by means of the CC equation. This agreement is due to the fact that the value of $T_{r,\max}$ is far from the critical point and near the acentric point ($T_r = 0.7$) chosen as reference to write the CC equation in the form of equation (4).

Using equations (1)–(3), we have analyzed the curvature of the 105 substances included in RefProp 9.0 and listed in table 1, in the reduced temperature range from $T_{r,tp} = T_{tp}/T_c$ to $T_r = 0.95$, T_{tp} being the triple-point temperature. For each fluid, the curvature presents a maximum at a different reduced temperature $T_{r,\max}$ reported in the third column in table 1. The curvature for CO_2, cyclopropane, propyne and SF_6 does not present a maximum. In the cases of CO_2 and SF_6 this absence is because their triple point reduced temperature is larger than 0.7. In the cases of cyclopropane and propyne the absence of a maximum in the curvature comes from numerical problems with the data reported in RefProp 9.0 for these fluids [3].

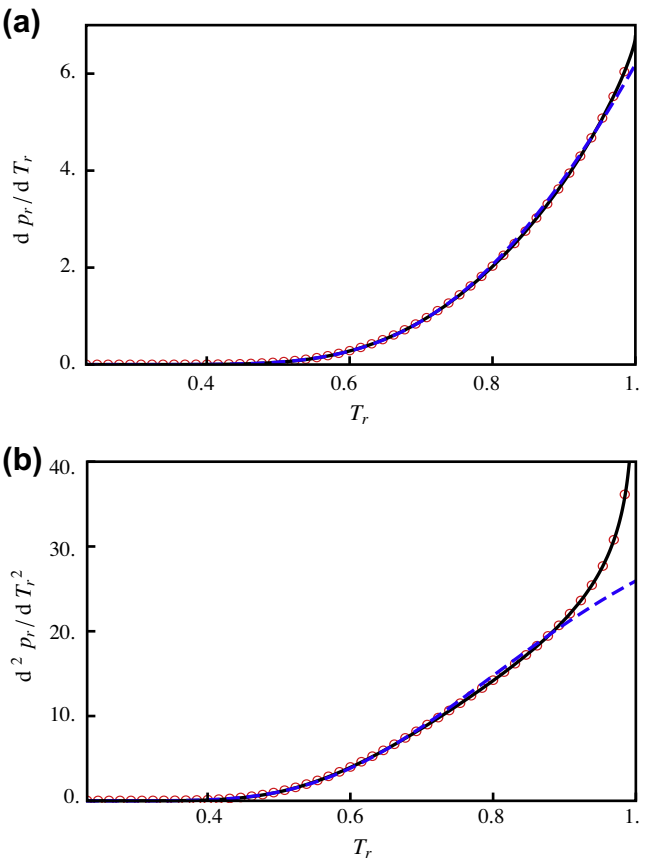

FIGURE 1. (a) Plot of the first derivative of the reduced vapor pressure dp_r/dT_r vs. the reduced temperature T_r for propane. (b) Plot of the second derivative of the reduced vapor pressure d^2p_r/dT_r^2 vs. T_r for propane. The solid lines represent equation (12) in (a) and equation (13) in (b), the dashed lines represent equation (7) in (a) and equation (8) in (b), in all cases $\omega = 0.1521$. The symbols are the values obtained from RefProp 9.0 [3] (see text).

Figure 3(a) shows a plot of $T_{r,\max}$ vs. ω. Symbols correspond to NIST data using the third column in table 1 and the dashed line corresponds to the maximum of the curvature of the CC vapor pressure equation, given by equation (9). We can see a fair agreement between NIST and CC values of $T_{r,\max}$. The average absolute relative deviation (AARD) between NIST and CC data for all fluids is 0.72%. The maximum absolute relative deviation (MARD) is obtained for MDM3M with a value of 1.47%.

Perhaps, the most widely recognized vapor pressure equation used in the literature for correlating vapor pressure experimental data of pure fluids with very good accuracy from the triple to the critical point is the Ambrose–Walton (AW) equation [6],

$$\ln p_r = \phi_0(T_r) + \omega\,\phi_1(T_r) + \omega^2\,\phi_2(T_r), \tag{10}$$

where the functions $\phi_k(T_r)$ ($k = 0, 1, 2$) have the form of a Wagner vapor pressure equation

$$\phi_k(T_r) = \frac{1}{T_r}\left[A_k(1-T_r) + B_k(1-T_r)^{1.5} + C_k(1-T_r)^{2.5} + D_k(1-T_r)^5\right], \tag{11}$$

where the twelve coefficients A_k, B_k, C_k and D_k ($k = 0, 1, 2$) take the same values for any fluid and are given in table 2. From equations (10) and (11) one obtains

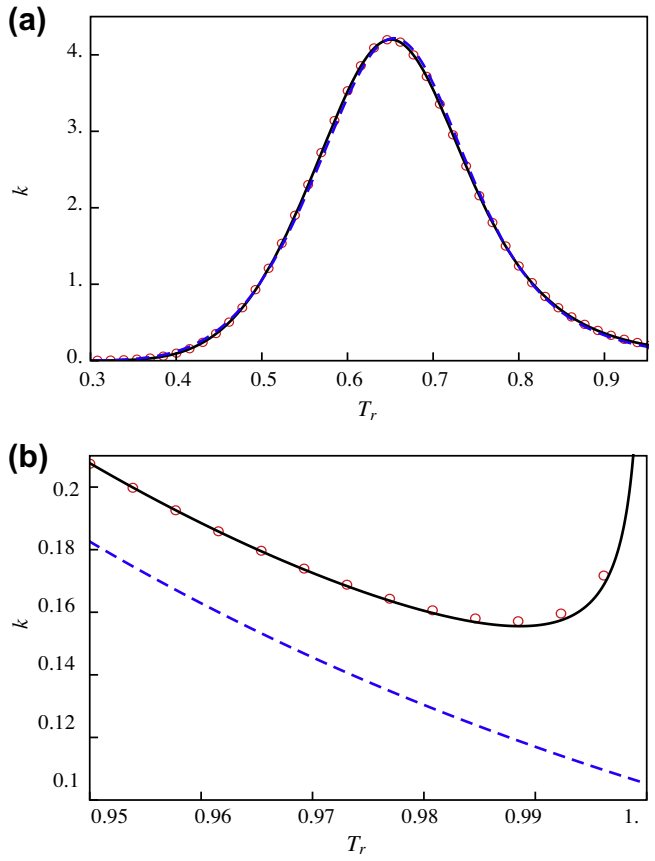

FIGURE 2. Plots of the curvature k vs. T_r for propane in different reduced temperature ranges. (a) $0.3 \leqslant T_r \leqslant 0.95$. (b) $0.95 \leqslant T_r < 1$. The solid lines represent the AW result, given by equation (1) with equations (12) and (13), the dashed lines represent the CC result given by equation (9), in all cases $\omega = 0.1521$. The symbols are the values obtained from RefProp 9.0 [3] (see text).

$$\frac{dp_r}{dT_r} = [\phi_0'(T_r) + \omega\,\phi_1'(T_r) + \omega^2\,\phi_2'(T_r)]p_r \tag{12}$$

and

$$\frac{d^2p_r}{dT_r^2} = [\phi_0''(T_r) + \omega\,\phi_1''(T_r) + \omega^2\,\phi_2''(T_r)]p_r + [\phi_0'(T_r) + \omega\,\phi_1'(T_r) + \omega^2\,\phi_2'(T_r)]^2 p_r, \tag{13}$$

with p_r given by equation (10) and

$$\phi_k'(T_r) = -\frac{1}{T_r}\left[A_k + \frac{3}{2}B_k(1-T_r)^{0.5} + \frac{5}{2}C_k(1-T_r)^{1.5} + 5D_k(1-T_r)^4\right] - \frac{\phi_k(T_r)}{T_r} \tag{14}$$

and

$$\phi_k''(T_r) = \frac{1}{T_r}\left[\frac{3}{4}B_k(1-T_r)^{-0.5} + \frac{15}{4}C_k(1-T_r)^{0.5} + 20D_k(1-T_r)^3\right] - \frac{2\phi_k'(T_r)}{T_r}. \tag{15}$$

The first and second derivatives of the reduced vapor pressure for propane ($\omega = 0.1521$) using equations (12) and (13) are plotted by solid lines in figure 1(a) and (b), respectively. One can see an excellent agreement between NIST and AW results.

TABLE 1
Critical temperature T_c , acentric factor ω, reduced temperature at which the curvature attains its maximum value $T_{r,\max}$, and reduced temperature at which the curvature attains its minimum value $T_{r,\min}$ obtained from RefProp 9.0[3] for the 105 fluids considered in this work (see main text).

Fluid	T_c (K)	ω	$T_{r,\max}$	$T_{r,\min}$
1-Butene	419.29	0.192	0.6574	0.9873
Acetone	508.1	0.3071	0.6772	0.9911
Ammonia	405.4	0.256	0.6695	
Argon	150.69	−0.0022	0.6185	0.9874
Benzene	562.02	0.211	0.6603	0.9903
Butane	425.12	0.201	0.6599	0.9896
Dodecane	658.1	0.574	0.7104	0.9896
Methylcyclohexane	572.2	0.23	0.6643	0.9953
cis-Butene	435.75	0.202	0.6591	0.9902
Propylcyclohhexane	630.8	0.33	0.6786	
Perfluorobutane	386.33	0.374	0.6846	0.9854
Perfluoropentane	420.56	0.423	0.6937	0.9885
Trifluoroiodomethane	396.44	0.18	0.6555	0.9855
Carbon monoxide	132.86	0.0497	0.6297	0.9853
Carbon dioxide	304.13	0.2239		0.9887
Carbonyl sulfide	378.77	0.0978	0.6399	0.9825
Cyclohexane	553.64	0.2093	0.66	0.9851
Cyclopentane	511.69	0.195	0.6586	0.9956
Cyclopropane	398.3	0.1305		0.9868
Deuterium	38.34	−0.175	0.5686	
Heavy water	643.85	0.364	0.6866	0.9876
D4	586.49	0.592	0.7097	0.9924
D5	619.23	0.658	0.7182	
D6	645.78	0.736	0.7264	0.9924
Decane	617.7	0.4884	0.7004	0.9942
DMC	557.38	0.3333	0.6806	
DME	400.38	0.196	0.6579	0.9934
Ethane	305.32	0.0995	0.6407	0.9878
Ethanol	513.9	0.644	0.7183	
Ethylene	282.35	0.0866	0.6376	0.988
Fluorine	144.41	0.0449	0.629	0.9805
Hydrogen sulfide	373.1	0.1005	0.6405	0.9859
Helium	5.2	−0.385	0.4834	0.979
Heptane	540.13	0.349	0.6823	
Hexane	507.82	0.299	0.675	
Hydrogen	33.15	−0.219	0.5587	0.9825
Isobutene	418.09	0.193	0.6576	
Isohexane	497.7	0.2797	0.6719	
Isopentane	460.35	0.2274	0.6637	0.9877
Isobutane	407.81	0.184	0.6558	0.9887
Krypton	209.48	−0.0009	0.6189	
MD2M	599.4	0.668	0.7205	0.993
MD3M	628.36	0.722	0.7233	0.9947
MD4M	653.2	0.836	0.7343	
MDM	564.09	0.529	0.7037	0.9909
Methane	190.56	0.0114	0.6221	0.9868
Methanol	513.38	0.5625	0.7125	0.9868
Methyl linoleate	799.	0.805	0.7341	
Methyl linolenate	772.	1.14	0.7662	
MM	518.7	0.418	0.6909	0.9836
Methyl oleate	782.	0.91	0.7449	
Methyl palmitate	755.	0.91	0.7466	
Methyl stearate	775.	1.02	0.7563	
Nitrous oxide	309.52	0.1613	0.6519	0.985
Neon	44.49	−0.0387	0.6111	0.9814
Neopentane	433.74	0.1961	0.6578	0.9861
Nitrogen trifluoride	234.	0.126	0.6525	0.9849
Nitrogen	126.19	0.0372	0.6274	0.9881
Nonane	594.55	0.4433	0.6947	
Octane	569.32	0.393	0.6883	
Orthohydrogen	33.22	−0.219	0.5594	0.9898
Oxygen	154.58	0.0222	0.6243	0.9885
Parahydrogen	32.94	−0.219	0.5592	0.9818
Pentane	469.7	0.251	0.6676	0.988
Propane	369.89	0.1521	0.6505	0.9879
Propylene	364.21	0.146	0.6493	0.9877
Propyne	402.38	0.204		0.9888
R11	471.11	0.1888	0.6572	0.9822
R113	487.21	0.2525	0.6675	0.9856
R114	418.83	0.2523	0.6683	
R115	353.1	0.25	0.6669	0.9842

(*continued on next page*)

TABLE 1 (*continued*)

Fluid	T_c (K)	ω	$T_{r,\max}$	$T_{r,\min}$
R116	293.03	0.2566	0.6683	0.9882
R12	385.12	0.1795	0.6555	0.9845
R123	456.83	0.2819	0.6721	0.9863
R1234yf	367.85	0.276	0.672	0.9878
R1234ze	382.52	0.313	0.6773	0.9887
R124	395.42	0.2881	0.6731	0.9885
R125	339.17	0.3052	0.6757	0.9868
R13	302.	0.1723	0.654	0.9842
R134a	374.21	0.3268	0.6792	0.9881
R14	227.51	0.1785	0.6554	0.983
R141b	477.5	0.2195	0.6618	0.9849
R142b	410.26	0.2321	0.6643	0.9871
R143a	345.86	0.2615	0.6698	0.9872
R152a	386.41	0.2752	0.6722	0.9857
R161	375.3	0.217	0.6629	
R21	451.48	0.2061	0.6599	0.9888
R218	345.02	0.3172	0.6774	
R22	369.3	0.2208	0.6636	0.9875
R227ea	374.9	0.357	0.6833	0.9873
R23	299.29	0.263	0.67	0.9876
R236ea	412.44	0.3794	0.6855	
R236fa	398.07	0.3772	0.6851	
R245ca	447.57	0.3536	0.6828	0.9821
R245fa	427.16	0.3776	0.6855	0.9891
R32	351.26	0.2769	0.673	0.9871
R365mfc	460.	0.38	0.6873	0.991
R41	317.28	0.2004	0.6609	0.9868
RC318	388.38	0.3553	0.6824	0.9877
Sulfur hexafluoride	318.72	0.21		0.989
Sulfur dioxide	430.64	0.2557	0.6681	0.9874
trans-Butene	428.61	0.21	0.6611	0.9874
Toluene	591.75	0.2657	0.67	
Water	647.1	0.3443	0.6834	0.9875
Xenon	289.73	0.0036	0.6199	0.9866

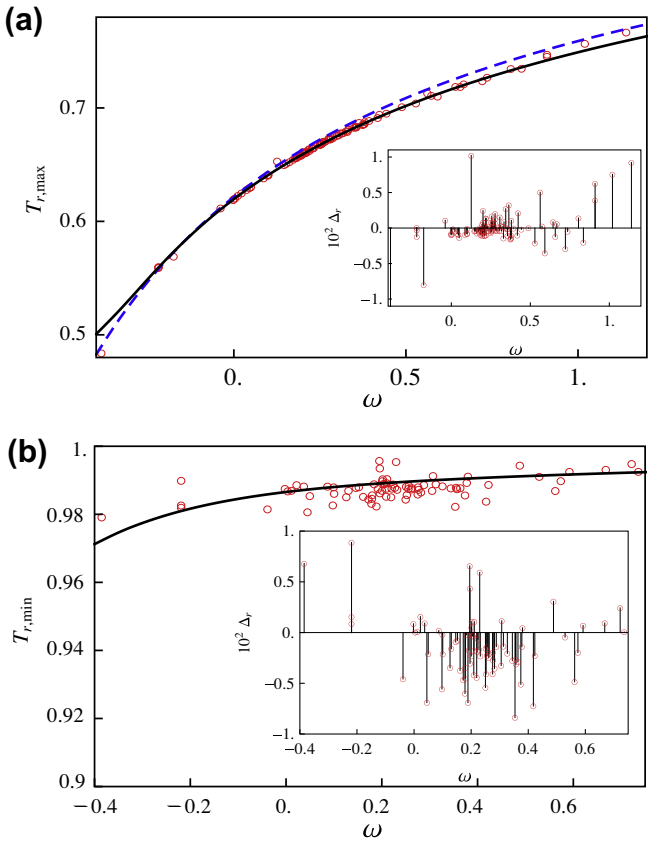

FIGURE 3. (a) The reduced temperature at which the curvature attains its maximum value $T_{r,\max}$ vs. the acentric factor ω. (b) The reduced temperature at which the curvature attains its minimum value $T_{r,\min}$ vs. the acentric factor ω. The solid lines are obtained from the AW equation. The dashed line in (a) represents the CC result. The symbols are the values obtained from RefProp 9.0 [3] for the 105 fluids considered in this work (see text). The insets show the percent relative deviations between AW and RefProp 9.0 data

The curvature for propane ($\omega = 0.1521$) using equation (1) with the first and second derivatives of the AW equation, given by equations (12) and (13), is also plotted in figure 2(a) by a solid line in the reduced temperature range $0.3 \leqslant T_r \leqslant 0.95$. This curvature presents a maximum at $T_{r,\max} = 0.6507$, very close to the value obtained from NIST data. The reduced temperature of the maximum of the curvature of the AW vapor pressure equation vs. ω is also plotted in figure 3(a) by a solid line. We can see an excellent agreement between NIST and AW values of $T_{r,\max}$, except for ^{4}He. Percent relative deviations ($10^2\Delta_r$) between NIST and AW data are shown in the inset of figure 3(a). The AARD between NIST and AW data for all fluids is 0.17%. The MARD is obtained for ^{4}He with a value of 4.49%. We ascribe this deviation to the lack of accuracy of the AW equation for the vapor pressure of ^{4}He.

3. Curvature near the critical point

At the critical point, the first derivative of the reduced vapor pressure w.r.t. the reduced temperature takes a fluid-dependent finite value,

$$\left(\frac{dp_r}{dT_r}\right)_{T_r=1} = \alpha_c, \tag{16}$$

usually named Riedel's factor [7]. In general, α_c increases with ω. For example, for the AW equation (10), using equations (12) and (14) one obtains,

$$\alpha_c^{AW} = -\left(A_0 + A_1\omega + A_2\omega^2\right), \tag{17}$$

with A_0, A_1 and A_2 given in table 2. Therefore, for ω values in the range $-0.4 \leqslant \omega \leqslant 1$, typical of the fluids here considered, equation (17) yields α_c values in the range $4 \leqslant \alpha_c \leqslant 12$.

TABLE 2
Coefficients for the Ambrose–Walton vapor pressure equation, equations (10) and (11) [6].

k	A_k	B_k	C_k	D_k
0	−5.97616	1.29874	−0.60394	−1.06841
1	−5.03365	1.11505	−5.41217	−7.46628
2	−0.64771	2.41539	−4.26979	3.25259

On the other hand, as one approaches the critical point, renormalization group theory establishes that the second derivative of the reduced vapor pressure w.r.t. the reduced temperature diverges following the scaling law [8]

$$\frac{d^2p_r}{dT_r^2} \approx B(1 - T_r)^{-\alpha}, \tag{18}$$

where α is the critical exponent for the heat capacity at constant volume and B is a fluid dependent positive coefficient. Taking into account equations (17) and (18), the curvature (1) must diverge following the scaling law

$$k \approx \frac{B}{\left(1 + \alpha_c^2\right)^{3/2}}(1 - T_r)^{-\alpha}, \tag{19}$$

when T_r approaches 1 (critical point). In other words, the curvature k and d^2p_r/dT_r^2 present the same kind of divergence at the critical point.

The CC equation (4) does not satisfy the scaling law (18) and, therefore, using equation (9) its curvature takes a finite value at the critical point given by

$$k_c^{CC} = \frac{A(\omega)[A(\omega)-2]}{\left[1+A(\omega)^2\right]^{3/2}}, \tag{20}$$

with $A(\omega)$ given by equation (5). The curvature for propane ($\omega = 0.1521$) obtained from the CC equation in the range $0.95 \leqslant T_r < 1$ is plotted by a dashed line in figure 2(b). One can see that the CC curvature decreases slowly towards the value $k_c^{CC} = 0.1052$ given by equation (20). On the contrary, equations (13) and (15) show that the AW equation satisfies the scaling law (18) with an effective critical exponent $\alpha = 0.5$. Therefore, the curvature of the AW equation also satisfies the scaling law (19) with an exponent $\alpha = 0.5$. The curvature for propane ($\omega = 0.1521$) obtained from the AW equation in the range $0.95 \leqslant T_r < 1$ is plotted by a solid line in figure 2(b). One can see that the AW curvature presents a minimum at a reduced temperature $T_{r,\min} = 0.9886$ and then it quickly increases with T_r so that $k^{AW} \to \infty$ when $T_r \to 1$. Since the curvature for both the CC and AW equations has a similar bell-shaped form far enough the critical point, one can conclude that the occurrence of a minimum of the curvature near the critical point can be obtained from vapor pressure equations thermodynamically consistent with the scaling law (18). Therefore, the reduced temperature $T_{r,\min}$ of this minimum can be considered as a marker for the critical region in the sense that it delimits the transition from a regular behavior far the critical point (a bell-shaped form with a maximum) to a singular behavior near the critical point (a divergence prescribed by the renormalization group theory). The curvature for propane using equations (1)–(3) and $\Delta_v h$, v^g, v^l, c_{v2}^g and c_{v2}^l data obtained from RefProp 9.0 [3], in the reduced temperature range $0.95 \leqslant T_r < 1$ is plotted by symbols in figure 2(b), showing a minimum at $T_{r,\min} = 0.9879$, very close to the above reported value for the minimum of the curvature of the AW equation.

Assuming that the saturated vapor pressure of any real fluid must satisfy the scaling law (18), the curvature of its reduced vapor pressure curve must present a minimum near the critical point. Using equations (1)–(3), we have analyzed the curvature of the 105 substances included in RefProp 9.0 and listed in table 1, in the reduced temperature range $0.95 \leqslant T_r < 1$. We find that for most fluids the curvature presents a minimum at a different reduced temperature $T_{r,\min}$ reported in the fourth column of table 1. Figure 3(b) shows a plot of $T_{r,\min}$ vs. ω. Symbols correspond to NIST data using the fourth column of table 1 and the solid line corresponds to the minimum of the curvature of the AW vapor pressure equation, given by equation (9). We can see a fair agreement between NIST and AW values of $T_{r,\min}$. The AARD between NIST and AW data for those fluids is 0.27%. The MARD is obtained for Orthohydrogen with a value of 0.89%. We note the absence of a minimum of the curvature for 25 fluids from NIST data. This absence could be due to the fact that the equation of state used for the NIST program for obtaining vapor pressure data for such fluids might fail near the critical point.

4. Summary

To summarize, we have used the curvature of the reduced vapor pressure curve as an alternative way to analyze the shape of this curve. By using vapor–liquid data of 105 fluids reported in the NIST data base, we find that, far from the critical point, the curvature presents a bell-shaped form with a maximum at a fluid dependent reduced temperature $T_{r,\max}$ belonging to the interval 0.5–0.8 and increasing as the acentric factor ω increases. On the other hand, near the critical point, the curvature presents a minimum at a fluid dependent reduced temperature $T_{r,\min}$ that belongs to the interval 0.980–0.995. This minimum can only be predicted by considering adequate functional forms for the vapor pressure curve. This happens for vapor pressure equations for which the second derivative w.r.t. the reduced temperature diverges at the critical point. This is the case of the Ambrose–Walton equation, which provides a good agreement between theoretical values for both $T_{r,\max}$ and $T_{r,\min}$ and those obtained from NIST data.

Acknowledgment

S.V., M.J.S., and J.A.W. thank financial support by Ministerio de Educación y Ciencia of Spain under Grant FIS2009-07557.

References

[1] K. Srinivasan, Chem. Eng. J. 81 (2000) 63–67.
[2] C.N. Yang, C.P. Yang, Phys. Rev. Lett. 13 (1964) 303–305.
[3] E.W. Lemmon, M.L. Huber, M.O. McLinden, NIST standard reference database 23: reference fluid thermodynamic and transport properties-REFPROP, version 9.0, National Institute of Standards and Technology, Standard Reference Data Program, Gaithersburg, 2010.
[4] S. Velasco, J.A. White, J. Chem. Eng. Data 56 (2011) 1163–1166.
[5] K.S. Pitzer, D.Z. Lippmann, R.F. Curl, C.M. Huggins, D.E. Petersen, J. Am. Chem. Soc. 77 (1955) 3433–3440.
[6] D. Ambrose, J. Walton, Pure Appl. Chem. 61 (1989) 1395–1403.
[7] L. Riedel, Chem. Eng. Tech. 26 (1954) 83–89.
[8] H.E. Stanley, Introduction to Phase Transitions and Critical Phenomena, Oxford University Press, New York, 1971.

JCT 12-667